

Ahmed El-Rafei, Tobias Engelhorn, Simone Waerntges, Arnd Doerfler, Joachim Hornegger and Georg Michelson: Glaucoma Classification Based on Histogram Analysis of Diffusion Tensor Imaging Measures in the Optic Radiation. *Computer Analysis of Images and Patterns, Lecture Notes in Computer Science*, (Eds.: Pedro Real, Daniel Diaz-Pernil, Helena Molina-Abril, Ainhoa Berciano and Walter Kropatsch) Springer Berlin/Heidelberg 2011, Volume 6854, 529-536, DOI: 10.1007/978-3-642-23672-3_64

This is the author submitted version of an article whose final and definitive form has been published in *Computer Analysis of Images and Patterns, Lecture Notes in Computer Science* © 2011 Springer. The original publication is available at www.springerlink.com with DOI: 10.1007/978-3-642-23672-3_64. The copyrights of the publication are exclusive to © 2011 Springer.

Glaucoma Classification Based on Histogram Analysis of Diffusion Tensor Imaging Measures in the Optic Radiation

Ahmed El-Rafei^{1,4}, Tobias Engelhorn², Simone Wärtges³, Arnd Dörfler²,
Joachim Hornegger^{1,4}, and Georg Michelson^{3,4,5}

¹ Pattern Recognition Lab, Department of Computer Science,
ahmed.el-rafei@informatik.uni-erlangen.de,

joachim.hornegger@informatik.uni-erlangen.de,

² Department of Neuroradiology,

tobias.engelhorn@uk-erlangen.de,

arnd.doerfler@uk-erlangen.de,

³ Department of Ophthalmology,

simone.waerntges@uk-erlangen.de,

georg.michelson@uk-erlangen.de,

⁴ Erlangen Graduate School in Advanced Optical Technologies (SAOT),

⁵ Interdisciplinary Center of Ophthalmic Preventive Medicine and Imaging (IZPI),
Friedrich-Alexander University Erlangen-Nuremberg, Germany

Abstract. Glaucoma is associated with axonal degeneration of the optic nerve leading to visual impairment. This impairment can progress to a complete vision loss. The transsynaptic disease spread in glaucoma extends the degeneration process to different parts of the visual pathway. Most of glaucoma diagnosis focuses on the eye analysis, especially in the retina. In this work, we propose a system to classify glaucoma based on visual pathway analysis. The system utilizes diffusion tensor imaging to identify the optic radiation. Diffusion tensor-derived indices describing the underlying fiber structure as well as the main diffusion direction are used to characterize the optic radiation. Features are extracted from the histograms of these parameters in regions of interest defined on the optic radiation. A support vector machine classifier is used to rank the extracted features according to their discrimination ability between glaucoma patients and healthy subjects. The seven highest ranked features are used as inputs to a logistic regression classifier. The system is applied to two age-matched groups of 39 glaucoma subjects and 27 normal controls. The evaluation is performed using a 10-fold cross validation scheme. A classification accuracy of 81.8% is achieved with an area under the ROC curve of 0.85. The performance of the system is competitive to retina based classification systems. However, this work presents a new direction in detecting glaucoma using visual pathway analysis. This analysis is complementary to eye examinations and can result in improvements in glaucoma diagnosis, detection, and treatment.

Keywords: Classification, Diffusion Tensor Imaging, Optic Radiation, Glaucoma, Histogram, Visual System

1 Introduction

More than 60 million people around the world suffer from glaucoma. Bilateral blindness caused by glaucoma is estimated to affect more than 8 million people [1]. Glaucoma is accompanied by neurodegeneration of the axonal fibers in the optic nerve along with visual impairment. The development of glaucoma can result in complete blindness. The vision loss can not be restored. However, if glaucoma is detected in an early stage, its progression can be delayed or stopped. Therefore, early detection of glaucoma is necessary as well as novel treatment methods.

The conventional trend in glaucoma diagnosis is through eye examinations. Intraocular blood pressure, retinal nerve fiber layer thickness measured by optical coherence tomography (OCT), fundus images, and optic disc topography evaluated by Heidelberg retina tomograph (HRT) are examples of glaucoma relevant data examined by ophthalmologists to evaluate the glaucoma severity. Moreover, systems were developed based on the aforementioned data among others using various eye imaging modalities to screen, detect, and diagnose glaucoma [2, 3]. Despite the efficiency and high performance of the developed systems, they focus on the eye, specifically the retina, ignoring the largest part of the visual system represented by the cerebral visual pathway fibers within the brain. In addition, the mechanism of glaucoma progression and the functional or structural damage precedence [4] are still unresolved issues. Therefore, exploring the recently discovered possibilities offered by diffusion tensor imaging (DTI) [5] to reconstruct and characterize the fiber structure of the human white matter [6] can be a valuable addition to the glaucoma examination flow.

Recent studies addressed the visual system changes due to glaucoma. Garaci et al. [7] showed that a reduction in fiber integrity affecting different parts of the visual pathway as the optic nerve and optic radiation is correlated with glaucoma. Another study showed axonal loss along the visual pathway from the optic nerve through the lateral geniculate nucleus till the visual cortex in the presence of glaucoma [8]. These results suggest that the visual pathway analysis can be significant in detecting and diagnosing glaucoma.

In this article, we investigate the significance of DTI-derived parameters in the optic radiation for glaucoma detection. We propose a classification system based on statistical features derived from the histograms of the DTI indices. The optic radiation is first identified automatically using the authors' developed algorithm [9]. A specific region of interest (ROI) on the optic radiation is then manually delineated. The histograms of the DTI measures are calculated. The histograms' statistical features are extracted from the histograms of the DTI indices in the specified ROI. The features are evaluated using a support vector machine classifier for dimensionality reduction and the highest ranked features are used for classification. The system is trained and tested using 10-fold cross validation. Finally, the ability of the system to differentiate between normal subjects and glaucoma patients is evaluated.

2 Classification System

2.1 Diffusion Tensor Imaging

Diffusion-weighted imaging (DWI) brain scans were acquired using a 3T-MRI high field scanner (Magnetom Tim Trio, Siemens, Erlangen, Germany). The diffusion weighting gradients were applied along 20 non-collinear directions with a maximal b-factor of $1,000 \text{ s/mm}^2$. The scans were repeated four times and averaged to increase the signal to noise ratio (SNR) and to improve the quality of the images. The axial resolution was $1.8 \times 1.8 \text{ mm}^2$ with 5 mm slice thickness. The corresponding acquisition matrix size was 128×128 on a field of view (FoV) of $23 \times 23 \text{ cm}^2$. The acquisition sequence protocol was a single-shot, spin echo, echo planar imaging (EPI) with parameters: TR = 3400 ms, TE = 93 ms, and partial Fourier acquisition = 60%. The scans were complemented by a non-weighted diffusion scan with b-factor equals zero. The Gaussian modeling of the diffusion process within a voxel is represented by a 3×3 diffusion tensor. The diffusion tensors were calculated from the DWI-datasets. The eigenvalue decomposition of the diffusion tensors contained information about the principal diffusion direction and aspects of the diffusion process (degree of anisotropy, mean diffusion, etc). The diffusion tensors were spectrally decomposed. The obtained eigenvalues were used to calculate the mean (MD), radial (RD), and axial (AD) diffusivities in addition to the fractional anisotropy (FA) [10]. The eigenvector corresponding to the largest eigenvalue was regarded as the principal diffusion direction (PDD).

2.2 Optic Radiation Segmentation

The identification of the optic radiation was performed using the authors' previously developed algorithm [9]. The algorithm operated on the interpolated DTI-images to produce an automatic segmentation of the optic radiation. The drawbacks of the Euclidean space interpolation and analysis of diffusion tensors were avoided by the utilization of the Log-Euclidean framework [11]. The DTI-images were enhanced by applying an anisotropic diffusion filtering to the individual elements of the diffusion tensors. This increased the coherency within the fiber bundles while preserving their edges. Based on neurophysiological facts of the dominant diffusion direction in the optic radiation and its anatomical size relative to other fibers, the optic radiation was initially identified using a thresholding and connectivity analysis. Similarly, the mid brain was approximately identified to be used later for segmentation enhancement. A region-based segmentation with the initialization of the optic radiation from the previous step was performed by a statistical level set engine [12]. The level set segmentation was adjusted to work with the Log-Euclidean metric for extending the framework to Riemannian operations while maintaining the computational efficiency. The framework optimized the posterior probabilities of partitioning the brain image space into the optic radiation and the remaining parts of the brain. The probabilities were modeled by normal distributions of the diffusion tensors within each

of the two division parts. Finally, the outcome of the level set segmentation was adjusted based on the relative anatomical position between the optic radiation and the mid brain. This was done to remove the tracts anteriorly connected to the optic radiation (i.e., optic tracts). Further details on the segmentation system can be found in [9].

2.3 Region of Interest Selection

In this step, a region of interest defined on the segmented optic radiation was configured. The slice containing the optic radiation and clearly identifying the termination of the optic tracts in the lateral geniculate nucleus (LGN) region was located in all subjects. The automatic segmentation on the selected slice was examined by two DTI experts and the segmentation errors were manually corrected. Moreover, the connection of the optic radiation to the primary visual cortex was manually eliminated. This region is characterized by misleading reduced fractional anisotropy due to the limitation of the diffusion tensor in modeling the branching and crossing fibers [13]. The final processed optic radiation on the selected slice was the ROI used in the remaining analysis. Figure 1 shows an example of a selected ROI on a sample subject.

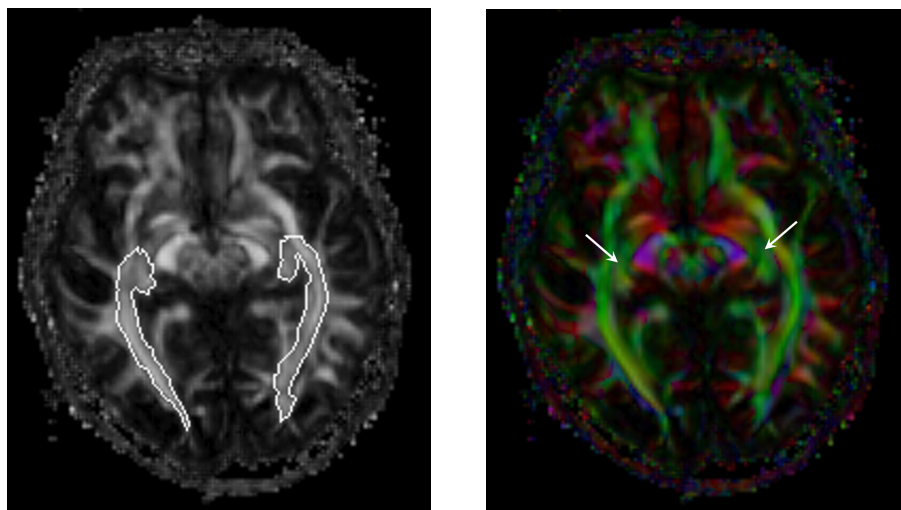


Fig. 1. The semi-automatically identified region of interest (ROI) representing the optic radiation shown on a fractional anisotropy image (left). The diffusion direction coded image (right) of the ROI-slice demonstrates the dominant anterior-posterior diffusion direction in the optic radiation. The selected slice indicates clearly the termination of the optic tracts at the lateral geniculate nuclei (LGN) as indicated by the white arrows on the right image.

2.4 Histogram Analysis and Feature Extraction

The histograms of the four DTI-derived parameters (FA, MD, RD, and AD) in the specified ROI were computed. A number of bins for each parameter were predetermined and the number of voxels corresponding to a certain bin range was calculated. The PDD has a unity length with three components representing the three coordinate axes. The PDD was converted to the spherical coordinate system. The histograms of the azimuth and inclination angles were measured by binning them in 0.2 radians bins. Since the sign of the PDD is not representative, the range of the azimuth angle was restricted between zero and 180 degrees while the inclination angle range was retained between zero and 180 degrees. That was simply done by inverting the direction of the PDD if it falls outside these ranges. Six first order statistical features (Mean, variance, skewness, kurtosis, energy, and entropy) of the DTI-indices and the PDD were derived from the histograms using the following equations:

$$Mean : \mu = \sum_{i=1}^N param(i) \times hist(i) \quad (1)$$

$$Variance : \sigma^2 = \sum_{i=1}^N (param(i) - \mu)^2 \times hist(i) \quad (2)$$

$$Skewness : \mu_3 = \sigma^{-3} \sum_{i=1}^N (param(i) - \mu)^3 \times hist(i) \quad (3)$$

$$Kurtosis : \mu_4 = \sigma^{-4} \sum_{i=1}^N (param(i) - \mu)^4 \times hist(i) - 3 \quad (4)$$

$$Energy : E = \sum_{i=1}^N [hist(i)]^2 \quad (5)$$

$$Entropy : H = - \sum_{i=1}^N hist(i) \log(hist(i)) \quad (6)$$

where N is the number of bins in the corresponding DTI-parameter histogram, $hist$ is the normalized histogram (i.e. probability distribution which is the histogram divided by the total number of voxels within the ROI), i is the index of the i^{th} bin, and $param(i)$ is the mean value of the corresponding parameter (param) in the i^{th} bin.

2.5 Feature Selection and Classification

A support vector machine classifier [14] was used to rank the 36 histogram features by recursive feature elimination. This procedure works as follows: The support vector machine classifier was trained using the complete feature set and

the features' weights were determined. Then, the feature with the lowest squared weight was considered as the least ranked feature. The feature with the lowest rank was removed from the feature set. The previous steps were repeated iteratively with the remaining features until all the features were ranked. The highest seven ranked features provided the best classification performance and were, therefore, selected as features for the classifier. For classification, the selected seven features were the input to a logistic regression classifier. The training and testing were performed using a 10-fold cross validation analysis. The software implementation in Weka [15] was used for the feature selection and the classification.

3 Results

The proposed system was applied to two groups of subjects: A group of 27 healthy controls with a mean age of 58.52 ± 10.10 years (17 females and 10 males) and 39 patients with primary open angle glaucoma (POAG) with a mean age of 61.74 ± 8.32 years (19 females and 20 males). The two groups were age matched and the two-sided Wilcoxon ranksum test which is equivalent to the Mann-Whitney U-test gave a p -value of 0.17 indicating the correlation between the ages of the two groups. The subjects underwent MRI and DTI brain scans. The brains were examined by experienced neuroradiologists and did not show any indications of neuronal diseases or lesions affecting the visual pathway. The optic radiations of all subjects were segmented and the ROIs were selected. The statistical features were extracted from the histograms of the four DTI-derived indices as well as the azimuth and inclination angles of the PDD. The features were ranked by a support vector machine classifier. The seven most discriminating features were: MD Kurtosis, RD Skewness, FA Entropy, MD Skewness, Azimuth Energy, Azimuth Entropy, and FA Mean, respectively. A logistic regression classifier was trained and tested using these seven features in a 10-fold cross validation setup.

The classification accuracy of the system was 81.82%. This rate corresponded to the correct recognition of 54 subjects' classes. Out of these 54 subjects, 36 were glaucoma patients and 18 were control subjects. Three glaucoma patients and 9 normal subjects were wrongly diagnosed. The receiver operating characteristic (ROC) curve was calculated and plotted in Figure 2. The area under the ROC curve was 0.853. A sensitivity of 92.31% for glaucoma detection and specificity of 70.37% were obtained. Additional values from the ROC curve at a different threshold showed a sensitivity of 71.79% at a fixed specificity of 85.19%.

4 Discussion and Conclusion

This paper proposed a new approach in glaucoma detection using visual pathway analysis. Utilizing the capabilities of the diffusion tensor imaging, the system identified and characterized the fiber structure of the optic radiation. First order statistical features extracted from the histograms of the DTI-derived measures

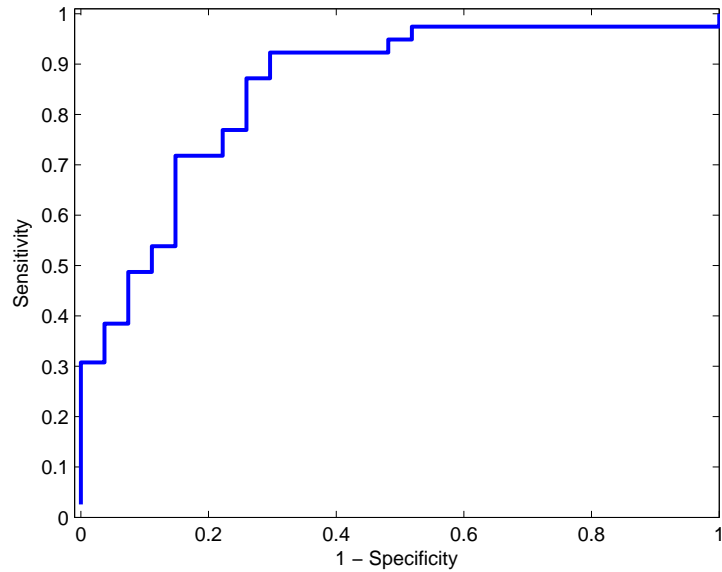


Fig. 2. The Receiver Operating Characteristic (ROC) curve of the glaucoma classification system based on DTI measures. The area under the ROC curve is 0.85.

were used to detect glaucoma. The classification performance obtained by the proposed system is comparable to systems based on eye imaging modalities [3]. Nevertheless, the significance of the DTI-parameters and the histogram features is evident from the limited number of features used.

Diffusion tensor-derived indices characterize different aspects of the underlying fiber structure. For example, FA indicates the degree of intravoxel fiber alignment and coherency while MD is related to the fiber integrity. Thus, these parameters were shown to correlate with the cerebral fiber damage caused by neuronal diseases such as Alzheimer and glaucoma. Four classification features among the highest ranked features were derived from the FA and the MD histograms demonstrating the sensitivity of these parameters to glaucoma. Fractional anisotropy and MD were shown to correlate with glaucoma [7] and such an influence can be expected.

The proposed classification method based on visual pathway analysis presents a new perspective in detecting diseases affecting the visual system such as glaucoma. Diffusion tensor imaging provides valuable information regarding the white matter microstructure allowing for the identification, characterization, and pathological diagnosis of fiber tracts. The high classification rates are indicators of the sensitivity of the features derived from the DTI-measures to glaucoma. It also emphasizes the effect of glaucoma on the entire visual system. This analysis is complementary to retina-based diagnosis. The integration of features from traditional eye imaging modalities and diffusion tensor imaging covers the complete visual system. Thus, it can enhance the detection of glaucoma significantly, the understanding of its pathophysiology, and consequently the treatment methods.

Acknowledgements

The authors gratefully acknowledge funding of the Erlangen Graduate School in Advanced Optical Technologies (SAOT) by the German National Science Foundation (DFG) in the framework of the excellence initiative.

References

- [1] Quigley, H.A., Broman, A.T.: The number of people with glaucoma worldwide in 2010 and 2020. *The British journal of ophthalmology* 890(3), 262-267 (2006)
- [2] Burgansky-Eliash, Z., Wollstein, G., Bilonick, R.A., Ishikawa, H., Kagemann, L., Schuman, J.S.: Glaucoma detection with the Heidelberg retina tomograph 3. *Ophthalmology* 114(3), 466-471 (2007)
- [3] Bock, R., Meier, J., Nyúl, L.G., Hornegger, J., Michelson, G.: Glaucoma risk index: Automated glaucoma detection from color fundus images. *Medical image analysis* 14(3), 471-481 (2010)
- [4] Hood, D.C., Kardon, R.H.: A framework for comparing structural and functional measures of glaucomatous damage. *Prog Retin Eye Res* 26(6), 688-710 (2007)
- [5] Basser, P.J., Mattiello, J., Lebihan, D.: MR diffusion tensor spectroscopy and imaging. *Biophysical Journal* 66(1), 259-267 (1994)
- [6] Staempfli, P., Rienmueller, A., Reischauer, C., Valavanis, A., Boesiger, P., Kollias, S.: Reconstruction of the human visual system based on DTI fiber tracking. *Journal of Magnetic Resonance Imaging* 26(4), 886-893 (2007)
- [7] Garaci, F.G., Bolacchi, F., Cerulli, A., Melis, M., Spanó, A., Cedrone, C., Floris, R., Simonetti, G., Nucci, C.: Optic nerve and optic radiation neurodegeneration in patients with glaucoma: in vivo analysis with 3-T diffusion-tensor MR imaging. *Radiology* 252(2), 496-501 (2009)
- [8] Gupta, N., Ang, L.C., de Tilly, L.N., Bidaisee, L., Yücel, Y.H.: Human glaucoma and neural degeneration in intracranial optic nerve, lateral geniculate nucleus, and visual cortex. *British Journal of Ophthalmology* 90(6), 674-678 (2006).
- [9] El-Rafei, A., Engelhorn, T., Waerntges, S., Doerfler, A., Hornegger, J., Michelson, G.: Automatic segmentation of the optic radiation using DTI in healthy subjects and patients with glaucoma. In: J.M.R.S. Tavares, R.M.N. Jorge (eds.) *Computational Vision and Medical Image Processing, Computational Methods in Applied Sciences* 19, Springer Netherlands, 1-15 (2011)
- [10] Basser P.J., Pierpaoli, C.: Microstructural and physiological features of tissues elucidated by quantitative-diffusion-tensor MRI. *Journal of magnetic resonance Series B*-111(3), 209-219 (1996)
- [11] Arsigny, V., Fillard, P., Pennec, X., Ayache, N.: Log-Euclidean metrics for fast and simple calculus on diffusion tensors. *Magn Reson Med* 56(2), 411-421 (2006)
- [12] Lenglet, C., Rousson, M., Deriche, R.: DTI segmentation by statistical surface evolution. *IEEE Transactions on Medical Imaging* 25(6), 685-700 (2006)
- [13] Tuch, D.S., Reese, T.G., Wiegell, M.R., Makris, N., Belliveau, J.W., Wedeen, V.J.: High angular resolution diffusion imaging reveals intravoxel white matter fiber heterogeneity. *Magnetic Resonance in Medicine* 48(4), 577-582 (2002)
- [14] Guyon, I., Weston, J., Barnhill, S., Vapnik, V.: Gene selection for cancer classification using support vector machines. *Machine Learning* 46(1-3), 389-422 (2002)
- [15] Hall, M., Frank, E., Holmes, G., Pfahringer, B., Reutemann, P., Witten, I.H.: The WEKA Data Mining Software: An Update. *SIGKDD Explorations* 11(1), 10-18 (2009)